

Polymethylene chain packing in epitaxially crystallized cycloalkanes: an electron diffraction study

Douglas L. Dorset

Electron Diffraction Department, Medical Foundation of Buffalo Inc., 73 High Street, Buffalo, NY 14203, USA

and Shaw-Ling Hsu

Polymer Science and Engineering Department, University of Massachusetts, Amherst, MA 01003, USA

(Received 14 June 1988; revised 10 January 1989; accepted 10 January 1989)

A new electron diffraction study is described for the cycloalkanes $c(\text{CH}_2)_{48}$, $c(\text{CH}_2)_{72}$ and $c(\text{CH}_2)_{96}$, adding structural information derived from epitaxially oriented samples to those already reported for solution grown microcrystals. In general the results are consistent with earlier diffraction and spectroscopic studies, i.e. the lower molecular weight cycloalkane packs in a non-orthorhombic subcell, whether grown from solution or from the melt (or epitaxially). Temperature of crystallization can determine whether this layer structure is oblique or rectangular; the latter high temperature form is perhaps metastable. Both the higher molecular weight cycloalkanes can crystallize in the orthorhombic subcell found for polyethylene but the $c(\text{CH}_2)_{72}$ crystallization may be induced by epitaxial nucleation. None of the diffraction patterns from epitaxially crystallized samples indicates lamellar ordering. At higher crystallization temperatures, where stem packing dominates over ordered chain folding, the preferred layer packing is rectangular, whether the subcell is monoclinic or orthorhombic.

(Keywords: crystal structure analysis; chain folding; polyethylene models)

INTRODUCTION

Although there are many types of evidence for chain folding in linear polyethylene lamellar crystals, the only structural studies which have produced quantitative spatial information about probable fold geometry at atomic resolution, as well as indicating the consequent strain induced to chain stem regions, have been the X-ray crystallographic analyses of cyclic alkanes. Thermal analyses^{1,2} have established that these cycloalkanes $c(\text{CH}_2)_n$ can be separated into at least three different classes, i.e. those where $12 \leq n \leq 24$, which have a mesomorphic phase transition well below the melting point, those for $24 \leq n \leq 48$, where no such transition takes place, and finally those with $n > 48$, for which the phase behaviour is dependent upon the method of crystallization. Representative crystal structures exist for the first two chain perimeter domains. In general, for compounds with $n > 21$, it is shown that when $n = 2u$, where u is an odd integer, the molecular packing in space group $P\bar{1}$ is very efficient so that the chain folds exert the least perturbation to the triclinic methylene subcell in the stem region^{3,4}. On the other hand, when $n = 2g$, where g is an even integer, the monoclinic crystal structure contains a perturbed triclinic stem subcell due to geometrical restrictions to chain folding not found in the $n = 2u$ structures^{3,5}.

In relation to the folding problem for linear polyethylenes, it is, of course, more interesting to investigate the structures of very large cycloalkanes for which the stem region would be permitted to pack in the

orthorhombic subcell most commonly found in the lamellar crystals of the infinite polymer. Although the largest cycloalkane crystal structure published to date is that of $c(\text{CH}_2)_{36}$, Trzebiatowski *et al.*⁵ also have shown that the crystal structures of $n = 12g$, where $g \equiv 0 \pmod{4}$, appear to be similar up to $c(\text{CH}_2)_{96}$, when these cycloalkanes are crystallized from solution. (A preliminary report of the $c(\text{CH}_2)_{48}$ crystal structure⁶ apparently supports this claim.) Powder X-ray⁶, spectroscopic^{2,7,8} and calorimetric² studies, on the other hand, indicate that the phase behaviour changes when these larger compounds are crystallized from the melt, i.e. the orthorhombic chain packing can then be identified for $c(\text{CH}_2)_{72}$ and $c(\text{CH}_2)_{96}$.

Recently⁶, an electron diffraction investigation of $c(\text{CH}_2)_{48}$, $c(\text{CH}_2)_{72}$ and $c(\text{CH}_2)_{96}$ was made to provide a more accurate description of the polymorphic behaviour of these compounds as crystallized from solution or from a melt. At least five crystalline forms were identified for the cycloalkanes, but only the $c(\text{CH}_2)_{96}$ was identified to pack in the orthorhombic form found for polyethylene, when solidified from the melt, in contrast to the earlier powder X-ray and spectroscopic data.

In this paper we describe another electron diffraction study of the same compounds in order to clarify the discrepancies between the previous studies on solution and melt crystallized samples. For this work we principally use samples which are epitaxially crystallized on an organic substrate to afford a view onto the molecular chains. This high energy crystallization is often

equivalent to crystallization from the melt. Some studies are also made of solution crystallized samples for comparison with recent work⁶ which considers a view more or less along the molecular chain axes.

THE METHYLENE SUBCELL CONCEPT

Before a meaningful discussion of the electron diffraction data can be given, a clear concept of the various possible modes of polymethylene chain packing must be given. As often used in the study of biological lipids and other alkane derivatives, the methylene subcell formulated by Vand and Bell⁹ and reviewed recently by Abrahamsson *et al.*¹⁰ is distinguished from the unit cell of a linear chain compound which may contain other features not included in the polymethylene packing volume (e.g. regions containing a functional group or, in the present instance, a molecular fold region). There is a reasonably small number of methylene subcells (see Reference 10 for three-dimensional representations) and the dominance of a diffraction pattern from an alkane derivative by their contribution can be used to advantage for *ab initio* phasing⁹, since their scattering patterns are easily recognized. Indeed, when electron diffraction intensities are obtained from a solution crystallized sample in a projection down a long unit cell axis, only the subcell pattern is most often seen, due to a diffraction incoherence caused by elastic crystal bend distortions¹¹. (On the other hand, because the unit cell projection is smaller, electron diffraction data from epitaxially oriented crystals of the same materials can be used to determine the total unit cell contents¹²).

In examples of cycloalkane crystal structures, then, both the unit cell and the methylene subcell of $c(\text{CH}_2)_{34}$ have triclinic symmetry⁴ and an orientation matrix can be defined to relate the subcell axes to the unit cell axes. For the crystal structures of $c(\text{CH}_2)_{36}$, on the other hand, the unit cell has monoclinic symmetry, whereas the methylene subcell is a deformed packing of the same triclinic structure found for the C_{34} homologue. A projection of this methylene subcell down the chain axes is shown in *Figure 1a* and the designation given by lipid crystallographers¹⁰ is T_{\parallel} , equivalent to the T subcell of Kitaigorodskii¹³. It can only exist for oblique layer packings, i.e. molecular layers where the chain axes are inclined to the layer surface normal.

A related methylene subcell is the monoclinic M of Kitaigorodskii¹³, termed M_{\parallel} by lipid crystallographers¹⁰, which is depicted in *Figure 1b*. Unlike the T_{\parallel} structure, where no planes can be drawn perpendicular to the chain axes to intersect simultaneously four adjacent methylene units at the cell edges, such a plane can be drawn for M_{\parallel} so that a rectangular layer structure (i.e. one where chain axes are not inclined to the surface normal), in addition to oblique layer structures, can be defined.

The methylene subcell found most often for polyethylene is the rectangular R of Kitaigorodskii¹³, termed O_{\perp} by lipid crystallographers¹⁰ and depicted in *Figure 1c*. It can be found in either rectangular layers or oblique layer chain packings. Its cylindrically averaged disorder structure is the 'rotator' phase of n-paraffins depicted in *Figure 1d* and designated H by both Kitaigorodskii¹³ and lipid crystallographers¹⁰. This is most commonly found in rectangular layer structures.

As stated above, electron diffraction data from solution or melt oriented samples are mostly useful for

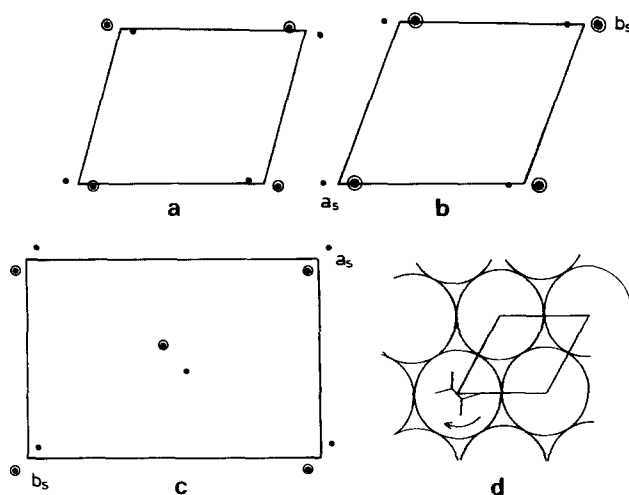


Figure 1 Methylene subcells¹⁰ considered in this work in projections down the chain axes; only carbon atoms are indicated. (a) Triclinic parallel T_{\parallel} , $a_s=4.285$, $b_s=5.414$, $c_s=2.539$ Å, $\alpha=80.99$, $\beta=112.2$, $\gamma=121.78^\circ$. Rings around the carbon atoms in the packing diagram indicate that these atoms are at nearly the same level (although in T_{\parallel} they cannot form a planar layer orthogonal to the chain axes.) Note the slipped arrangement of adjacent polymethylene chains. (b) Monoclinic parallel M_{\parallel} , $a_s=4.27$, $b_s=5.17$, $c_s=2.57$ Å, $\gamma=113.9^\circ$. While superficially resembling T_{\parallel} , the chains are oriented the same way along c_s to allow formation of a rectangular layer packing. (c) Orthorhombic perpendicular O_{\perp} , $a_s=7.47$, $b_s=4.95$, $c_s=2.54$ Å. (d) The hexagonal subcell H is a rotationally disordered form of O_{\perp} with $a_s=4.8$ Å, $\gamma=120^\circ$ (Hydrogen positions are added in this projection of a chain zig-zag)

determining the methylene subcell packing; the true unit cell may not be apparent in these data. As shown in studies of n-paraffins, however, the total unit cell symmetry can be determined with electron diffraction data from epitaxially crystallized samples and the intensity data can be used to determine the total crystal structure^{14,15}.

EXPERIMENTAL

Very small samples of three cycloalkanes; cyclooctatetracontane $c(\text{CH}_2)_{48}$, cyclodoheptacontane $c(\text{CH}_2)_{72}$ and cyclohexanonacontane, $c(\text{CH}_2)_{96}$, were obtained from Prof. G. Wegner, University of Freiburg, FRG and used without further purification. For crystallization from solution, small amounts were dissolved in hot *p*-xylene and a drop of the solution was allowed to evaporate on a carbon-film-covered electron microscope (e.m.) grid. Epitaxial crystallization was carried out by lattice matching on benzoic acid using the method of Wittmann *et al.*¹⁶. Briefly, a small amount of the *p*-xylene solution is allowed to evaporate on a freshly cleaved mica sheet. Carbon-film-covered e.m. grids are then placed face down over areas containing the thin film of the cycloalkane. Benzoic acid crystals are then scattered between these grids and the other mica sheet half is placed over this surface to make a sandwich. The sandwich is moved along a thermal gradient until the benzoic acid melts and the sample is then cooled to allow the benzoic acid to direct the epitaxial orientation of the cycloalkane as the eutectic line is reached. The mica sheets are separated, whereupon the benzoic acid is sublimed away *in vacuo* to leave oriented lath-like crystals of the cycloalkane (*Figure 2*) on the grid surface.

Selected area electron diffraction measurements were made at 100 kV with a Jeol JEM-100B electron

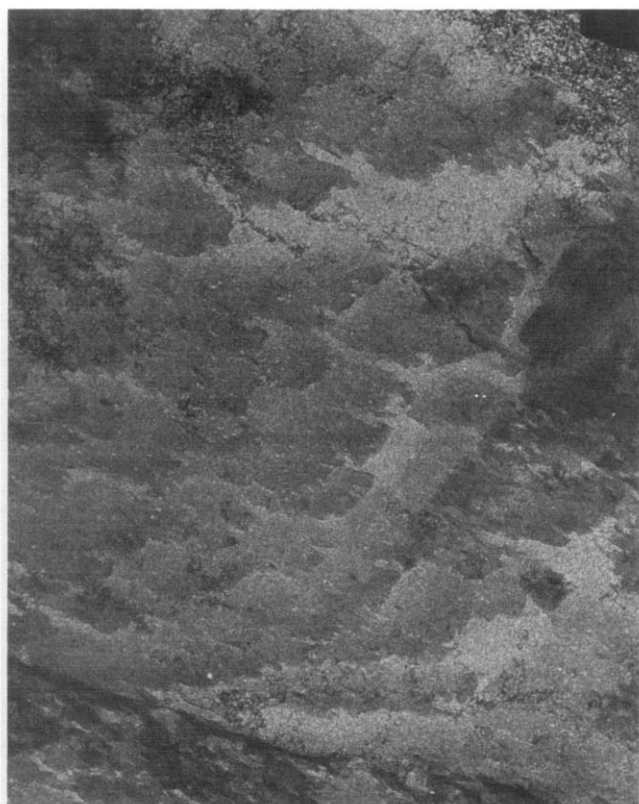


Figure 2 Lath-like microcrystals of cyclo $(\text{CH}_2)_{72}$ epitaxially crystallized on benzoic acid. By analogy with preliminary work on *n*-paraffins and polyethylene⁹, the long chain axes lie in the major crystal face, parallel to the narrowest lath edge

microscope. As usual¹⁷, care was taken to minimize radiation damage to the specimen by control of incident electron beam flux and choice of an adequately fast photographic emulsion (Kodak DEF-5 X-ray film) to permit rapid exposures to be taken. Camera lengths are calibrated with a gold Debye–Sherrer diagram. For melt recrystallization of solution grown microcrystals or general heating experiments on these samples, a Gatan 626 temperature-controlled specimen holder was utilized in the electron microscope, which is capable of holding selected temperatures in the range -170 to $+150^\circ\text{C}$.

For quantitative structure analysis, intensities were measured from scans of electron diffraction films with a Joyce Loebel MKIIC flatbed microdensitometer. The intensities were measured as triangular approximations of densitometer peak areas without further corrections for crystal texture (see Reference 17). Kinematic structure factor calculations based on known methylene subcell packings were done using Doyle–Turner electron scattering factors¹⁸.

Quantitative comparisons of diffraction data will be made below, but *Figure 3* illustrates the type of electron diffraction pattern expected from two rectangular layer packings of epitaxially oriented specimen if only the subcells, respectively M_{\parallel} and O_{\perp} , are contributing to the intensity data.

RESULTS

Cyclooctatetracontane, $c(\text{CH}_2)_{48}$

As shown in *Figure 4a*, electron diffraction data from solution crystallized samples indicate that the chain axes are not inclined to the surface normal, in contrast to the

major A polymorph characterized by Lieser *et al.*⁶, for which the chains are tilted by 27° . The crystal form, which persists to 80°C , resembles the B polymorph found in the earlier study. (We have not verified the existence of the higher temperature H subcell, termed D in their nomenclature.) Assuming the lower temperature form to be a monoclinic structure, we determine subcell parameters to be $a_s = 4.27$, $b_s = 5.17$, $c_s = 2.55 \text{ \AA}^*$, $\gamma = 113.9^\circ$, in agreement with values given for M_{\parallel} for lipid structures¹⁰. (These values also agree with the subcell dimensions given by Lieser *et al.*⁶ in their *Figure 8*.) A quantitative structure analysis considering the similar projections of T_{\parallel} and M_{\parallel} as alternative models is reviewed in *Table 1*. Neither structure can be distinguished in terms of crystallographic residual R. Nevertheless, since only M_{\parallel} permits a rectangular layer, this must be the subcell of this solution crystallized form. Electron diffraction patterns from epitaxially crystallized samples (*Figure 4b*) contain diffuse bands spaced at multiples of $(2.56 \text{ \AA})^{-1}$ along one axis with an axial reflection at $(1.28 \text{ \AA})^{-1}$ corresponding to I_{002} of the M_{\parallel} subcell. An orthogonal axial reflection at $(4.64 \text{ \AA})^{-1}$ corresponds to I_{010} of the same subcell. The third, off-axis, reflection at the same level is (011). Occasional interpenetration of several upper layer zones on one pattern is due to a typical elastic crystal bend deformation¹⁴. If the methylene subcell were T_{\parallel} , the axial reflections would lie on a non-orthogonal reciprocal lattice net instead of the orthogonal net found in this study. Note that there is no evidence of a (00ℓ) lamellar reciprocal lattice row in *Figure 4b*.

Cyclodoheptacontane $c(\text{CH}_2)_{72}$

An initial study of solution crystallized $c(\text{CH}_2)_{72}$ was complicated by the presence of a low melting

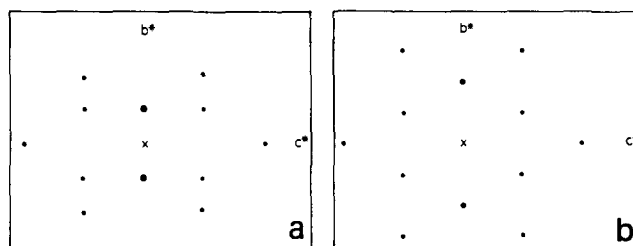


Figure 3 Simulated electron diffraction patterns in a projection onto the long chains, considering only subcell scattering: (a) $(0k\ell)$ pattern from the M_{\parallel} subcell (compare with *Figures 4b* and *5d*); (b) $(0k\ell)$ pattern from the O_{\perp} subcell (compare with *Figures 5e* and *6c*)

Table 1 Comparison of observed and calculated structure factors for a parallel chain subcell in solution crystallized $c(\text{CH}_2)_{48}$

$hk0$	$ F_0 $	F_c	
		M_{\parallel} subcell	T_{\parallel} subcell
100	3.11	+3.20	+3.04
200	1.40	+0.92	+0.89
010	2.42	+3.49	+3.46
020	0.70	+0.41	+0.10
110	1.40	+1.85	+0.95
$\bar{1}10$	3.11	+3.03	+3.64
120	1.40	+0.27	+1.69
210	1.37	+1.34	+0.97
220	0.84	+0.73	+1.00

*1 $\text{\AA} = 10^{-1} \text{ nm}$

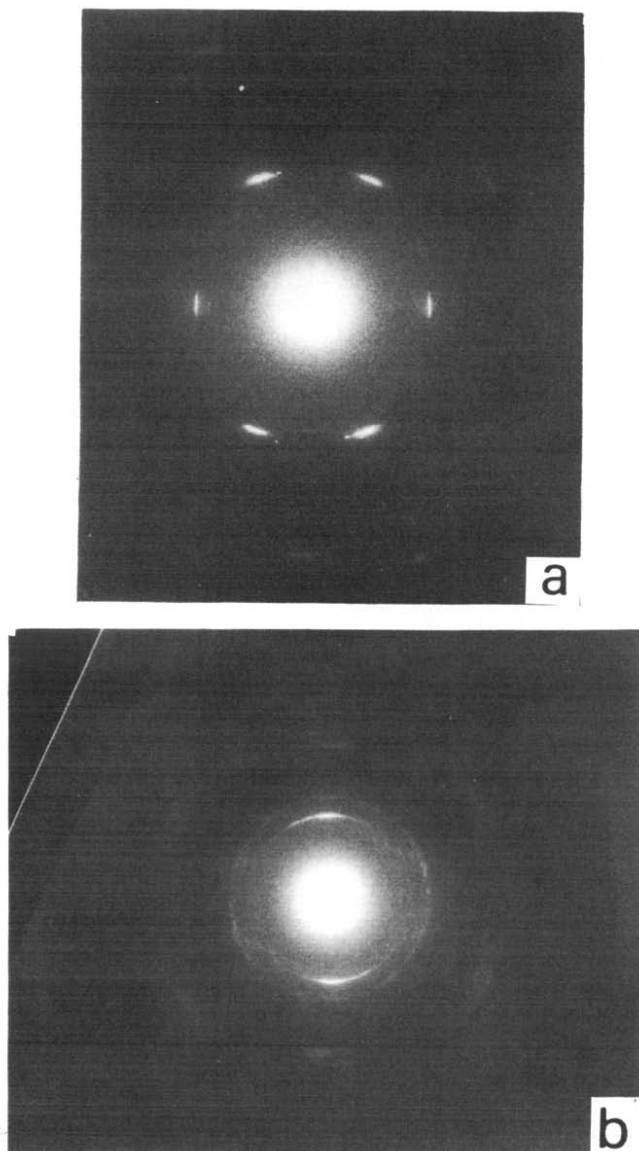


Figure 4 Electron diffraction patterns from cyclo $(\text{CH}_2)_{48}$. (a) Grown from hot *p*-xylene. The pattern is characteristic of either a M_{\parallel} or a T_{\parallel} subcell in a projection down the long chain axes. However, only the monoclinic subcell can exist for a rectangular layer. The cell dimensions are $d_{100} = 4.27$, $d_{010} = 5.27$ Å, $\gamma = 113.9^\circ$ and persist for crystals heated to 80°C . (b) Epitaxially grown crystal. Note that the $(0k\ell)$ pattern also represents a rectangular layer. Reflection indices also correspond well to major M_{\parallel} intensities. The measured orthogonal subcell dimension along the chain is 2.57 Å

contaminant (m.p. $\approx 56^\circ\text{C}$, as determined on the Gatan stage) which diffracts very much like untilted orthorhombic paraffin crystals. (Since electron diffraction is not an efficient technique for determining the bulk concentration of such a component, even a small amount of contaminant can be problematic if it crystallizes more readily than the sample being studied.) The actual electron diffraction pattern from the cycloalkane is shown in *Figure 5a* and resembles those obtained from even or odd chain triglycerides^{19,20}, for which polymethylene chains pack in the T_{\parallel} methylene subcell. When these crystals are heated beyond the melting point of the solution crystallized forms (107.0°C) and then recooled, diffraction patterns taken at 60°C resemble either those from the solution-grown crystals of $c(\text{CH}_2)_{48}$ (*Figure 5b*) or from the hexagonal methylene subcell¹⁰ (*Figure 5c*). This temperature was chosen to prevent the appearance of any low melting crystalline contaminant and also to

ensure that the $c(\text{CH}_2)_{72}$ crystals could be held above the pretransition found for the melt crystallized form.

Epitaxially crystallized samples produce two types of diffraction pattern. One pattern (*Figure 5d*) resembles *Figure 2b* with indices in accord with the M_{\parallel} subcell orientation discussed above (*Figure 3a*). The other pattern (*Figure 5e*), which is more frequently found, is a rectangular net with indices matching those from the O_{\perp} subcell¹⁰ (*Figure 3b*). In either case there are no 00ℓ reflections due to a lamellar repeat. When these epitaxially crystallized samples are heated to 60°C , it is still possible to find diffraction patterns similar to *Figures 5d* and *e*. After heating to 114°C and recoiling to 59°C , the only patterns found are rings with a spacing $d = 4.09 \pm 0.09$ Å, corresponding again to the hexagonal H subcell ('rotor' phase)²¹, which is not the somewhat expanded value for this dimension seen earlier⁶.

Cyclohexanonacontane $c(\text{CH}_2)_{96}$

The study of solution crystallized $c(\text{CH}_2)_{96}$ was complicated by a similar low melting contaminant to that found for $c(\text{CH}_2)_{72}$. However, Debye-Scherrer patterns could be obtained (*Figure 6a*) with strong reflections at $(4.62 \text{ \AA})^{-1}$, $(4.24 \text{ \AA})^{-1}$, $(3.91 \text{ \AA})^{-1}$ and $(3.65 \text{ \AA})^{-1}$. All but the second spacing can be shown to correspond to either T_{\parallel} or M_{\parallel} , depending on choice of representative unit cell axial lengths¹⁰. The second ring, which persists after the sample is heated to 94°C (*Figure 6b*) may be due to a (110) reflection in the expanded form of the O_{\perp} subcell²².

Results from the epitaxially crystallized samples, on the other hand, are unequivocal. It is clear that (*Figure 6c*) the material crystallizes in the O_{\perp} subcell, i.e. patterns strongly resemble those from similarly oriented and annealed polyethylene¹⁶. The match of the observed structure factors to calculated values is also shown in *Table 2* (see also the $0k\ell$ representation in *Figure 3b*). Even though these samples are well oriented, and exhibit crystal perfection, there is no sign of a lamellar spacing in the $0k\ell$ diffraction patterns.

When the solution grown samples are heated to 120°C (the melting point for this form is 115.9°C) and recooled, hexagonal diffraction patterns can be found when the sample is held at 79°C (*Figure 6d*). (Selection of this temperature avoids any influence from the unknown contaminant.)

DISCUSSION

A favourable comparison of our results with those reported by Lieser *et al.*⁶ can be made, especially when the differences in our experimental conditions are kept in mind. For example, a different solvent system was used in our study and, since the crystals were grown from hot solutions, crystal forms are expected to represent a higher energy polymorph, especially for the lowest molecular weight cycloalkane. Also, the epitaxial crystallization is carried out at high temperatures (i.e. near the melting point of benzoic acid), a condition again favouring higher energy polymorphic forms of e.g. *n*-paraffins¹⁵ than are crystallized from solution.

The smallest cycloalkane $c(\text{CH}_2)_{48}$ is only obtained as a rectangular layer structure in our hands, corresponding to the B form of Lieser *et al.*⁶, which is quantitatively identified here (*Table 1*) as the M_{\parallel} methylene subcell. To our knowledge this rectangular chain packing in M_{\parallel} for

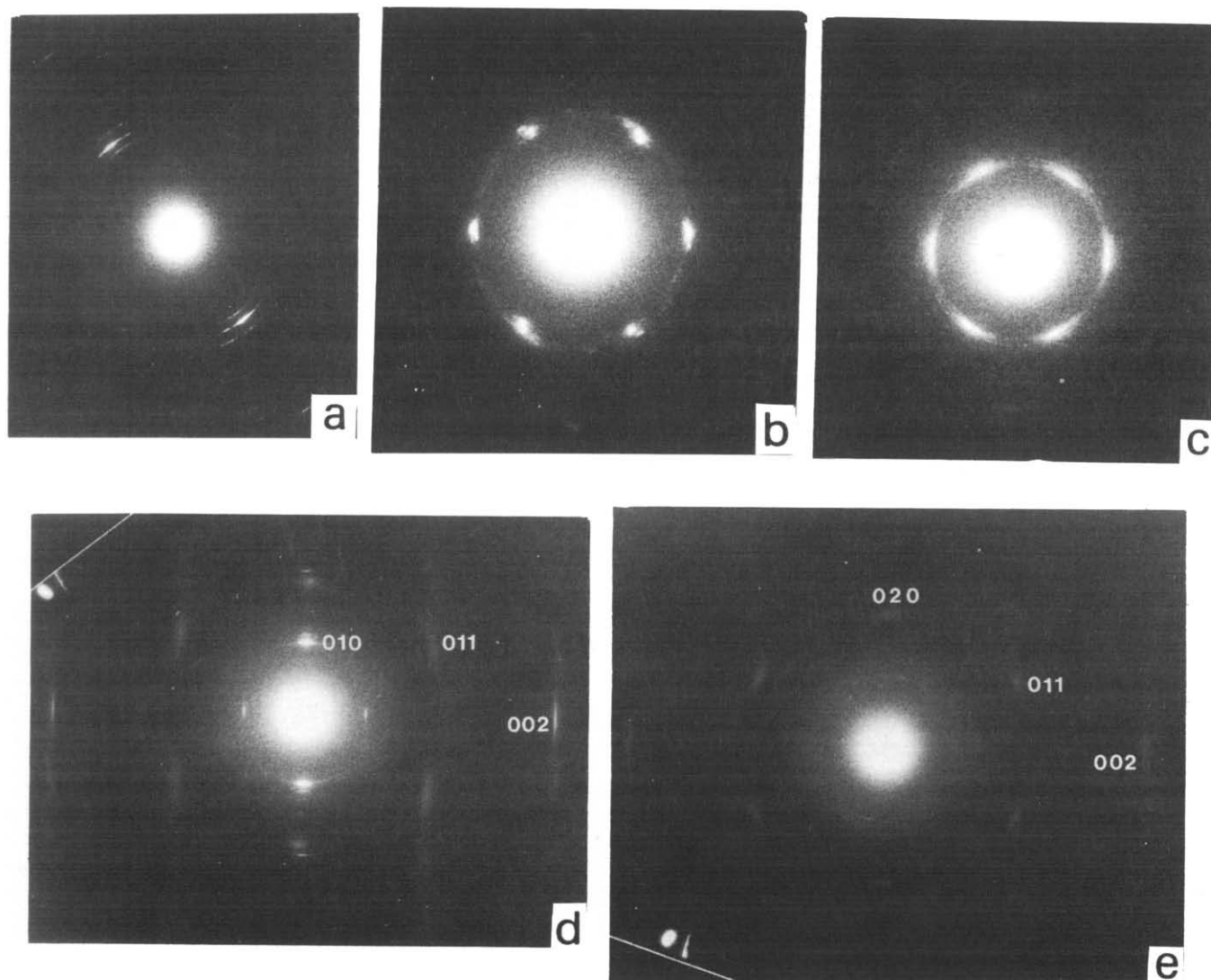


Figure 5 Electron diffraction patterns from cyclo $(\text{CH}_2)_{72}$. (a) Solution crystallized, representing an oblique chain pattern layer packing in the T_{\parallel} subcell. The intense lattice row is spaced at $(4.43 \text{ \AA})^{-1}$. (b) Crystallization from the melt. The pattern resembles that from $c(\text{CH}_2)_{48}$ (Figure 2a) and, from its symmetry, indicates that the chains are untilted. (c) Crystals cooled to 60° from the melt in the hexagonal methylene subcell. (d) Epitaxially crystallized sample with reflection indices corresponding to the M_{\parallel} subcell (see Figure 3a). (e) Epitaxial crystal in the O_{\perp} subcell. The smearing of the reflections along b^* is due to several types of crystal distortion, including in-plane curvilinear deformation of the crystal plate causing upper layer reflections to intersect the Ewald sphere

cycloalkanes is the first actual demonstrated non-oblique structure for this subcell, even though it has been theoretically predicted by Kitaigorodskii¹³. Our data do not exclude the possibility of the A polymorph which must pack in the T_{\parallel} subcell. This is because the oblique layer packing characterized earlier⁶ is almost identical to the chain orientation formed in electron diffraction studies of triglycerides^{19,20}, which also have a similarly oriented T_{\parallel} subcell and therefore similar diffraction patterns. The presence of the inclined chain T_{\parallel} packing is indicated in Figure 5a for $c(\text{CH}_2)_{72}$ and, as found earlier⁶, the untilted B form (we do not observe their C polymorph) in the M_{\parallel} subcell co-exists with the D form (H subcell) in samples grown from the melt. We see no evidence for the O_{\perp} subcell in melt crystallized samples but it is certainly evident when the material is epitaxially crystallized on benzoic acid, since it co-exists with the M_{\parallel} form. This perhaps illustrates a point made by Lieser *et al.* that their failure to observe their E-polymorph in the O_{\perp} subcell for $c(\text{CH}_2)_{72}$ is due to a lack of appropriate crystal nuclei. The lattice matching of benzoic acid

certainly can provide such nuclei (i.e. by matching the $d_{020} = 4.95 \text{ \AA}$ of the chain packing with the $b = 5.14 \text{ \AA}$ axis of the benzoic acid crystal structure), as shown by Wittmann *et al.*¹⁶.

The dominance of the O_{\perp} subcell, or E polymorph, is evident in epitaxially crystallized $c(\text{CH}_2)_{96}$ and the $0k\ell$ intensity data agree well with expected values for polyethylene. We see no evidence, however, for the O_{\perp} polymorph in melt crystallized samples; only the hexagonal subcell is found. It should be pointed out that the electron diffraction pattern shown earlier⁶ for the E form does not correspond to the O_{\perp} subcell either, but actually appears to be due to a rotationally deformed polymorph which has not quite transformed to H. A similar pattern has been obtained from an ether analogue of a triglyceride²³. Identification of the previously given polymorphs⁶ in terms of commonly used subcell notations is reviewed in Table 3.

One especially surprising finding from our studies is that, despite the observation of lamellar reflections for solution or melt crystallized cycloalkanes in earlier

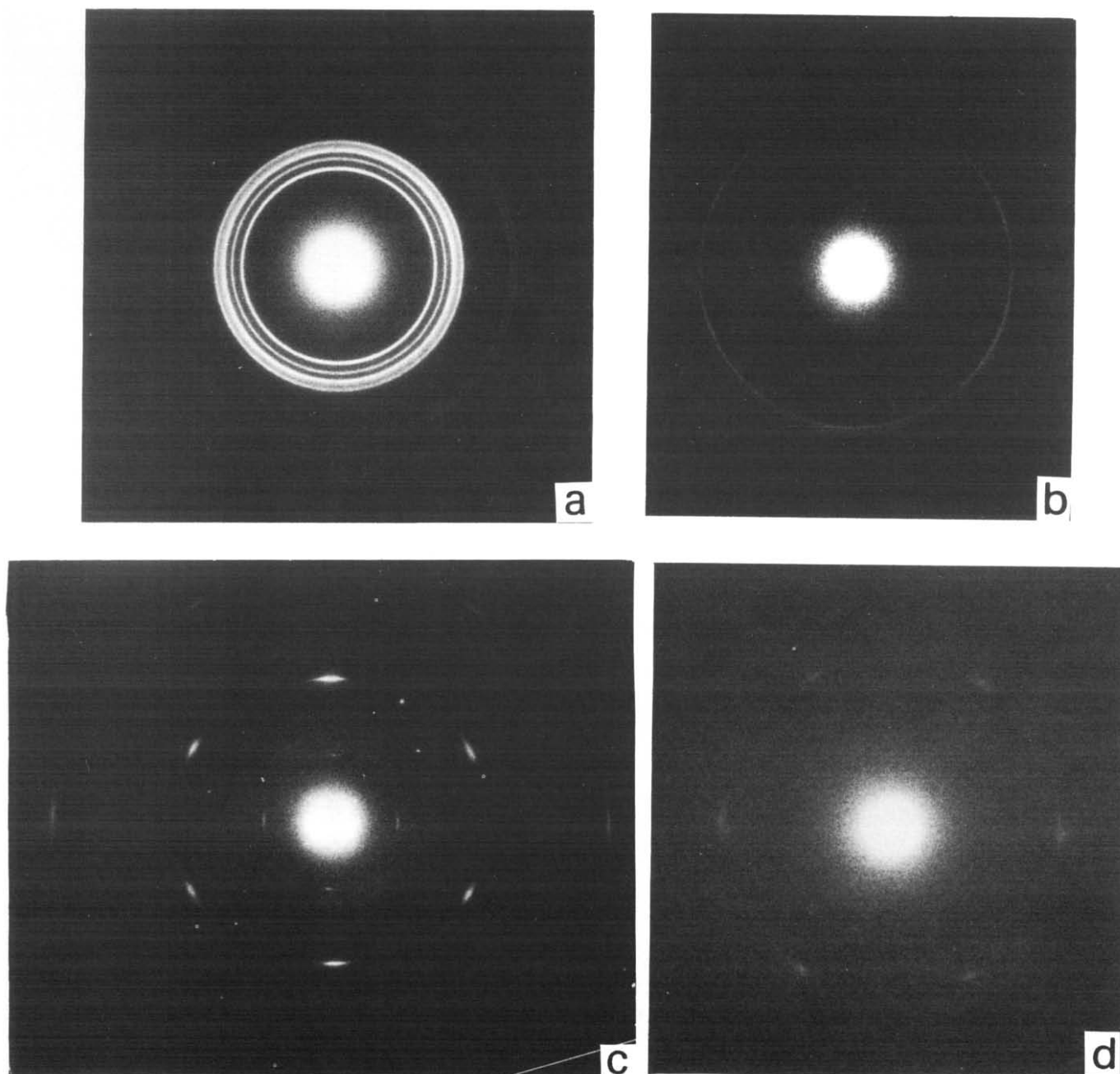


Figure 6 Electron diffraction pattern from cyclo $(\text{CH}_2)_{96}$. (a) Debye-Scherrer pattern from solution grown crystals. (b) Ring pattern with reflection at $(4.24 \text{ \AA})^{-1}$ left after heating solution grown crystal to 94°C . (c) Epitaxially crystallized sample in a well ordered O_\perp methylene subcell (compare with *Figure 3b*). (d) Sample recrystallized from the melt and held at 79°C . The pattern is characteristic of the hexagonal methylene subcell

Table 2 Comparison of O_\perp subcell structure factors for epitaxially crystallized $c(\text{CH}_2)_{96}$

$Ok\ell$	$ F_o $	F_c
002	0.87	-0.73
011	1.12	-1.45
020	1.55	-1.68
031	0.75	-0.68
040	0.32	-0.06

work^{5,6}, we see no such reflections in electron diffraction data from epitaxially crystallized samples. Only subcell reflections are seen, despite the fact that unit cell diffraction patterns are clearly observed from epitaxially oriented normal alkanes^{14,15} and other linear molecules. From model calculations made to explain similar

Table 3 Assignment of conventional subcell terminology to polymorphic crystal forms of cycloalkanes identified by Lieser *et al.*⁶

Polymorph designation ⁶	Subcell	
	Abrahamsson ¹⁰	Kitaigorodskii ^{1,3}
A	T_\parallel	$T[\frac{1}{2}, 1]$
B	M_\parallel	$M[0, 0]$
C	—	—
D	H	$H[0, 0]$
E	O_\perp	$R[0, 0]$

patterns from n-alkanes vapour-deposited on a cold nucleating substrate²⁴ this indicates that the lamellar ordering is severely disrupted, perhaps by random nematic-type longitudinal chain slips, while the register

of the chain zig-zag is preserved. Thus, it is significant that, when cycloalkanes are crystallized at high temperatures so that an ordered stem packing is preferred over ordered chain-fold and lamellar packing, an untilted chain layer is found to be present. On the other hand, when low temperature crystallization from solution is carried out, the whole lamellar structure, including folds, is ordered, and then oblique layer packings are found in this chain perimeter range, even though the higher energy rectangular form may be seen more frequently for the higher molecular weight species⁶. Energetically speaking, this implies that the chain twist imposed by the unfavourable fold geometry of $c(\text{CH}_2)_{2g}$ cycloalkanes (see above) only can be compensated adequately by a sufficiently long stem length. The importance of this finding for polyethylene should be even more apparent after a study of larger members of this series.

ACKNOWLEDGEMENTS

Research described in this paper was supported by NSF grant DMR86-10783. Dr J. C. Wittmann and Dr B. Lotz are thanked for discussions of this work.

REFERENCES

- 1 Grossmann, H. P. *Polym. Bull.* 1981, **5**, 137
- 2 Drotloff, H., Emeis, D., Waldron, R. F. and Möller, M. *Polymer* 1987, **28**, 1200
- 3 Groth, P. *Acta Chem. Scand.* 1979, **A33**, 199
- 4 Kay, H. F. and Newman, B. A. *Acta Crystallogr.* 1968, **B24**, 615
- 5 Trzebiatowski, T., Dräger, M. and Strobl, G. R. *Makromol. Chem.* 1982, **183**, 731
- 6 Lieser, G., Lee, K. S. and Wegner, G. *Colloid Polym. Sci.* 1988, **266**, 419
- 7 Lee, K.-S., Wegner, G. and Hsu, S. L. *Polymer* 1987, **28**, 889
- 8 Grossmann, H. P., Arnold, R. and Bürkle, K. R. *Polym. Bull.* 1980, **3**, 135
- 9 Vand, V. and Bell, I. P. *Acta Crystallogr.* 1951, **4**, 465
- 10 Abrahamsson, S., Dahlen, B., Löfgren, H. and Pascher, I. *Prog. Chem. Fats Other Lipids* 1978, **16**, 125
- 11 Dorset, D. L. *Ultramicroscopy* 1983, **12**, 19
- 12 Moss, B., Dorset, D. L., Wittmann, J. C. and Lotz, B. *J. Macromol. Sci. Phys.* 1985-1986, **B24**, 99
- 13 Kitaigorodskii, A. I. 'Organic Chemical Crystallography', Consultants Bureau, NY, 1961, pp. 181-192
- 14 Moss B., Dorset, D. L., Wittmann, J. C. and Lotz, B. *J. Polym. Sci., Polym. Phys. Edn.* 1984, **22**, 1919
- 15 Dorset, D. L. *J. Polym. Sci., Polym. Phys. Edn.* 1986, **24**, 79
- 16 Wittmann, J. C., Hodge, A. M. and Lotz, B. *J. Polym. Sci., Polym. Phys. Edn.* 1983, **21**, 2495
- 17 Dorset, D. L. *J. Electron. Microsc. Technol.* 1985, **2**, 89
- 18 Doyle, P. A. and Turner, P. S. *Acta Crystallogr.* 1968, **A24**, 390
- 19 Buchheim, W. *Kiel. Milchwirtsch. Forschungsber.* 1970, **22**, 3
- 20 Dorset, D. L. *Z. Naturforsch.* 1983, **38c**, 511
- 21 Dorset, D. L., Moss, B., Wittmann, J. C. and Lotz, B. *Proc. Natn. Acad. Sci. USA* 1984, **81**, 1913
- 22 Sundell, S. *Acta Chem. Scand.* 1977, **A31**, 799
- 23 Dorset, D. L. and Pangborn, W. A. *Chem. Phys. Lipids* 1982, **30**, 1
- 24 Dorset, D. L. and Zhang, W. P. unpublished results